

SceneCompleter: Dense 3D Scene Completion for Generative Novel View Synthesis

Weiliang Chen², Jiayi Bi², Yuanhui Huang¹, Wenzhao Zheng^{1,*}, Yueqi Duan^{2†}

Department of Automation, Tsinghua University, China

Department of Electronic Engineering, Tsinghua University, China

{cw124, bijy22, huangyh22}@mails.tsinghua.edu.cn; wenzhao.zheng@outlook.com;

duanyueqi@tsinghua.edu.cn

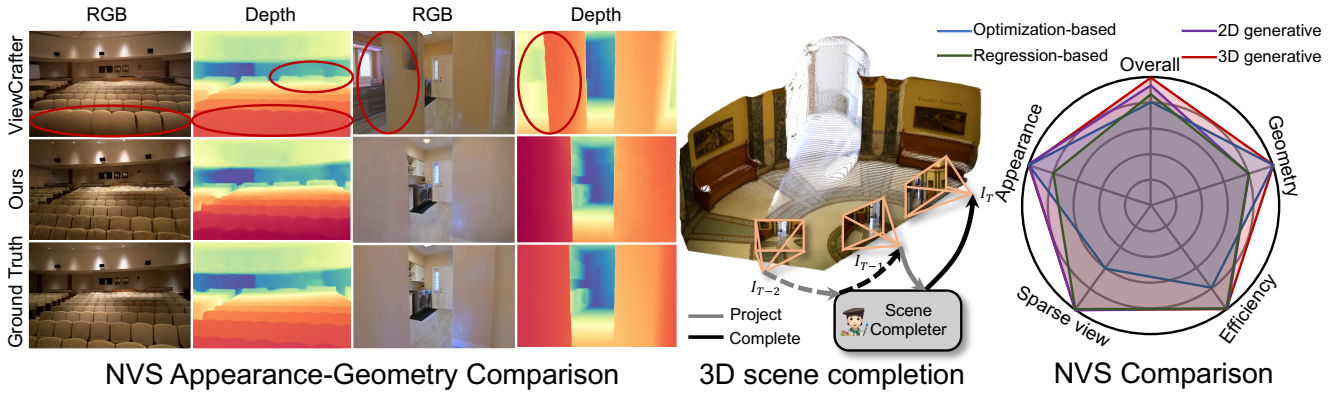


Figure 1. **SceneCompleter** explores 3D scene completion for generative novel view synthesis. By jointly modeling geometry and appearance, and incorporating geometry information into the generative process, SceneCompleter enables geometrically consistent and visually compelling novel view synthesis. With SceneCompleter, we can iteratively complete 3D scenes, ensuring both appearance and structure are accurately restored.

Abstract

Generative models have gained significant attention in novel view synthesis (NVS) by alleviating the reliance on dense multi-view captures. However, existing methods typically fall into a conventional paradigm, where generative models first complete missing areas in 2D, followed by 3D recovery techniques to reconstruct the scene, which often results in overly smooth surfaces and distorted geometry, as generative models struggle to infer 3D structure solely from RGB data. In this paper, we propose **SceneCompleter**, a novel framework that achieves 3D-consistent generative novel view synthesis through dense 3D scene completion. SceneCompleter achieves both visual coherence and 3D-consistent generative scene completion through two key components: (1) a geometry-appearance dual-stream diffusion model that jointly synthesizes novel views in RGBD space; (2) a scene embedder that encodes a more holis-

tic scene understanding from the reference image. By effectively fusing structural and textural information, our method demonstrates superior coherence and plausibility in generative novel view synthesis across diverse datasets. Project Page: <https://chen-wl20.github.io/SceneCompleter/>

1. Introduction

Novel view synthesis (NVS) has gained significant attention in computer vision due to its broad applications in virtual reality [4], 3D content creation [15, 18, 19], autonomous driving [1, 9, 20, 36] and beyond. The core challenge lies in inferring 3D structure and appearance from limited views while generating plausible and visually coherent novel views. Despite achieving promising results with powerful differentiable 3D representations [11, 21], optimization-based methods rely on dense multi-view inputs to dynamically search for the 3D structure, posing challenges in both efficiency and practical application.

¹Project Leader

²Corresponding Author

Recently, regression-based methods [2, 3] have explored feedforward novel view synthesis, directly regressing pixel-aligned 3D representation parameters from sparse views. Despite showing promising results for nearby viewpoints through scene priors learned from large-scale training data, the ill-posed nature of the problem causes these methods to produce unsatisfactory artifacts and unrealistic geometry when applied to other viewpoints. Pioneered by Zero-1-to-3 [18], research [5, 15, 35] has begun to explore generative novel view synthesis using powerful generative models. These methods typically involve synthesizing novel views with image or video generation models [7, 23, 26, 33], followed by estimating the 3D structure from the generated views for downstream reconstruction. However, the implicit nature of performing novel view synthesis in pixel space makes it challenging for these methods to infer 3D structure, leading to distorted geometry. For example, in a projected incomplete view of a hall as shown in Figure 1, a 2D generative model might fill in overly smooth chair backs in the missing areas, while overlooking the armrests. This may happen because the armrests of the chairs occupy much less area than the backs, causing the model to interpolate the appearance of the chair backs in the missing areas. However, in 3D space, the small area of the chair armrests holds greater geometric significance, offering 3D clues for novel view synthesis.

In this paper, we introduce SceneCompleter, a novel framework that leverages dense 3D scene completion to enable geometry-consistent generative novel view synthesis. The core insight is that geometry information is crucial in generative novel view synthesis, as the model needs to infer the 3D structure of the scene and extrapolate to generate the missing area. Therefore, simultaneously modeling geometry and appearance is crucial for generative novel view synthesis. Specifically, we first extract the geometry and appearance clues from the reference view with a powerful stereo reconstruction model Dust3R [30]. Then we design a Geometry-Appearance Dual-stream Diffusion model to perform generative novel view synthesis in 3D geometry-appearance space (A, G) . By jointly modeling geometry and appearance, this approach enables the generation of geometrically plausible novel views. Additionally, we introduce a Scene Embedder that encodes the overall scene information from the reference view to guide generation, which plays a crucial role in addressing the highly ill-posed problem of large-angle viewpoint changes. After recovering the completed geometry and appearance, we propose a simple yet effective alignment strategy to seamlessly integrate the completed 3D structure with the original, ensuring a more coherent and accurate reconstruction. Extensive experiments demonstrate that our method enables zero-shot novel view synthesis with both appearance and geometric consistency across multiple datasets.

2. Related Work

Regression-based Novel View Synthesis. Conventional approaches in Novel View Synthesis (NVS) relies on dense multi-view images as inputs to learn the 3D representation of the target scene in an optimization manner [8, 21, 22], suffering from inefficiency and limited applicability in practical scenarios. Leveraging the fast rendering speed of 3D Gaussians [11], a series of works [2, 3, 32] have shifted toward a new regression-based pipeline, which extracts scene priors from large datasets. These methods directly regress pixel-aligned 3D Gaussian parameters from sparse input views, demonstrating excellent interpolation results and high efficiency when synthesizing novel views close to the reference view. However, the ill-posed nature of this approach causes significant issues when dealing with large viewpoint changes, leading to unrealistic results. In this paper, we explore generative novel view synthesis by using generative models to complete the missing 3D structure in sparse views, thus enabling realistic novel view synthesis even with large viewpoint changes.

Generative Novel View Synthesis. With the rapid advancement of generative models [7, 25] and their impressive results, leveraging these models to synthesize novel views offers a natural solution to the challenge of missing viewpoints. Pioneered by Zero-1-to-3 [18], researchers have begun exploring generative models [17, 19, 27] for novel view synthesis, framing it as a conditional generation task. However, these approaches primarily focus on object-level novel view synthesis for downstream 3D content creation. MotionCtrl [31] and CameraCtrl [6] extend this idea by synthesizing novel views through video generation models, taking a reference image and a camera trajectory as input to generate a sequence of novel view videos. However, since the image itself lacks scale information, the model struggles to learn accurate camera trajectories, making it difficult to generate perspective-correct novel views. Recently, ViewCrafter [35] and ReconX [16] have addressed this limitation by leveraging video generation for novel view synthesis. They employ a powerful pretrained stereo reconstruction model to project the reference view onto the target view before generation, inherently resolving the scale issue. However, they still focus on 2D image completion while overlooking geometric cues, which can lead to inconsistent 3D structures. In this paper, we explore 3D generative novel view synthesis by jointly modeling geometry and appearance for dense 3D scene completion, enabling 3D-consistent novel view synthesis.

Dense 3D Scene Reconstruction. Based on the powerful 3D pointmap representation, Dust3R [30] initiates a trend toward dense 3D scene reconstruction without relying on traditional camera models. Subsequently, Mast3R [13] further introduces a local feature for each pixel-aligned point to achieve a better performance. These works require

post-processing and global alignment when reconstructing dense scenes from multiple inputs, as they only establish spatial matching between two views. To overcome this, Spann3r [29] and Fast3r [34] achieve dense 3D scene reconstruction directly from multiple images by maintaining a spatial memory of past frames or further expanding the original network. However, these works only operate in a discriminative manner, densely reconstructing the scene based on as many visual inputs as possible. In this paper, we guide this dense reconstruction network to provide unified geometry clues for generative 3D scene completion and then achieve the ultimate novel view synthesis.

3. Proposed Approach

In this section, we introduce **SceneCompleter**, a novel framework that leverages dense 3D scene completion to achieve geometrically consistent generative novel view synthesis. We first outline the motivation behind SceneCompleter in Section 3.1. Then, we describe the *Geometry-Appearance Clue Extraction* process in Section 3.2. Next, we introduce the *Geometry-Appearance Dual-Stream Diffusion* module in Section 3.3 and the *Scene Embedder Module* in Section 3.4. Finally, we present our *Geometry Alignment and Scene Completion* strategy in Section 3.5. An overview of our framework is illustrated in Figure 2.

3.1. Motivation of Our SceneCompleter

The goal of Novel View Synthesis (NVS) is to reconstruct a set of target views $\{I_i\}_{i=1}^N$ at corresponding camera poses $\{P_i\}_{i=1}^N$, given a limited set of input views $\{I_i\}_{i=1}^M$ with poses $\{P_i\}_{i=1}^M$, where $M = 1, 2, 3, \dots$. Fundamentally, this requires recovering a 3D scene (A, G) that simultaneously satisfies both camera pose and image constraints, where A represents the appearance and G denotes the geometry. The problem becomes highly ill-posed when M is small, especially when $M = 1$, making it naturally suited for a conditional generative modeling approach, as adopted in recent methods [16, 35]. However, these approaches primarily focus on completing A , emphasizing RGB completion while struggling to infer the underlying 3D structure. Consequently, they often generate unrealistic geometry and visually inconsistent renderings, as illustrated in Figure 1. To this end, we reformulate the problem as a dense 3D scene completion task, where both A and G are jointly completed. This enables the model to better infer the underlying 3D structure, leading to more plausible novel view synthesis.

3.2. Geometry-Appearance Clue Extraction

3D geometry construction. To jointly model (A, G) , we first need to reconstruct the 3D structure from the reference views, which provides the geometric clues for subsequent conditional generation. Specifically, we leverage the powerful unconstrained stereo 3D reconstruction method

Dust3R [30] to construct our 3D geometry clues. Given the input images $\{I_i\}_{i=1}^N$, Dust3R first constructs a connectivity graph $G(V, E)$, where the N images form vertices V , and each edge $e = (n, m) \in E$ indicates that images I^n and I^m share some visual content. It then estimates the pointmap for each pair of images and performs global alignment to obtain the final pointmap $\{X_i\}_{i=1}^N$.

Geometry clue extraction. The most intuitive idea would be to use the pointmap as geometry clues. However, two key challenges arise. First, the structure of the pointmap is unstructured and implicit, which is dissimilar to RGB images, making it challenging for the model to establish and learn the correspondence between them. Second, utilizing the pointmap as geometry clues introduces the challenge of aligning coordinate systems, which complicates its subsequent application. To address these challenges, we instead choose depth as a more suitable geometry clue, as depth maps do not have the coordinate system issue and are visually similar to RGB images, making the correspondence easier to learn. Therefore, for a novel viewpoint I_i , we project the pointmap into a depth map using the camera parameters K_i , R_i , and T_i as follows:

$$\mathbf{p}_i = K_i [R_i | T_i] \mathbf{X}_i, \quad (1)$$

$$d = \frac{1}{p_i^z}, \quad (2)$$

where p_i^z represents the z-coordinate of the projected point. The resulting depth map d serves as the geometry clue, which is then used for subsequent processing.

3.3. Geometry-Appearance Dual-stream Diffusion

Our goal is to achieve dense 3D scene completion, and the key challenge lies in how to incorporate geometry G into the completion process. To address this challenge, we design a depth encoder-decoder that maps the depth map to a latent space, and combine it with a Geometry-Appearance dual-stream U-Net to simultaneously complete both appearance and geometry information in the latent space. Our model builds on Stable Diffusion 2 [25], pretrained on the large-scale LAION-5B [28] dataset, leveraging its strong priors for natural images.

Depth encoder and decoder. A straightforward approach to encoding both depth and image into the latent space is to modify the channel dimensions of the diffusion model’s variational autoencoder (VAE). However, this disrupts the powerful priors that the pretrained diffusion model has learned for natural images. Instead, we employ two separate VAEs to encode depth and image independently. For the depth VAE, we replicate the depth map three times and stack them to match the three-channel input requirement of the VAE. To address the issue of numerical scale differences between images and depthmaps, we apply an

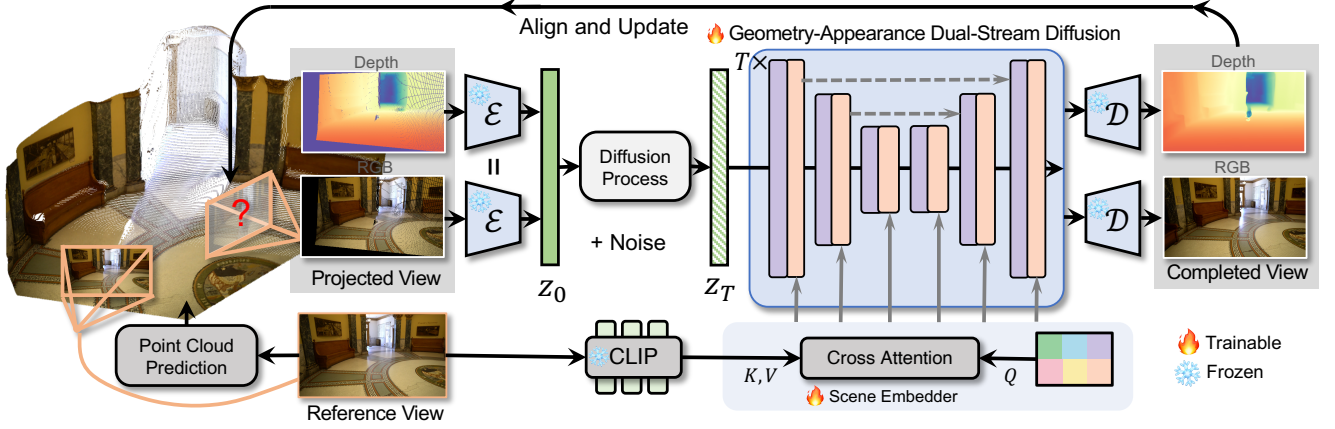


Figure 2. **Framework of SceneCompleter.** We first extract the geometry-appearance clues from the reference view using an unconstrained stereo reconstruction method. Then, we employ a Geometry-Appearance Dual-Stream Diffusion model to generate novel view in 3D space, conditioned on the extracted geometry-appearance clues. After generating the 3D novel view, we align the synthesized geometry with the original 3D structure to achieve 3D scene completion. Notably, this process can be iterated to progressively generate a larger 3D scene.

affine-invariant depth normalization, formulated as:

$$d_n = \left(\frac{d - d_2}{d_{98} - d_2} - 0.5 \right) \times 2, \quad (3)$$

where d and d_n represent the depth map before and after normalization, and d_2 and d_{98} denote the 2nd and 98th percentile values of the depth map, respectively. Demonstrated by Marigold [10], this processing enables the original VAE to reconstruct depth almost losslessly. Therefore, we utilize two weight-sharing VAEs to separately encode and decode depth and image without any fine-tuning:

$$z_d = \mathcal{E}(d_n), \quad \hat{d} = \mathcal{D}(z_d), \quad (4)$$

$$z_i = \mathcal{E}(I), \quad \hat{I} = \mathcal{D}(z_i), \quad (5)$$

where z_d and z_i are the latent codes for depth and image, respectively, and \mathcal{E} and \mathcal{D} are the encoder and decoder. \hat{d} and \hat{I} are the reconstructed depth and image.

Geometry-appearance denoising Unet. To achieve simultaneous completion of geometry and appearance (A, G), we perform generation in the 3D space of image and depth. Specifically, we apply the diffusion forward process in the RGBD space and predict the noise in the RGBD space. We first concatenate the image and depth latent codes z_i and z_d to obtain z_0 . During the noise-adding process, we add noise to z_0 as follows:

$$z_t = \sqrt{\alpha_t} z_0 + \sqrt{1 - \alpha_t} \epsilon, \quad (6)$$

where $\epsilon \sim \mathcal{N}(0, I)$, $\alpha_t := \prod_{s=1}^t (1 - \beta_s)$, and $\{\beta_1, \dots, \beta_T\}$ is the variance schedule for the process with T steps. The variable $t \in \{1, \dots, T\}$ represents the noising steps. For the incomplete appearance and geometry clues I_p and d_p , we use the corresponding encoder \mathcal{E} to transform them into

their respective latent representations $z_{i,p}, z_{d,p}$, which are then concatenated with z_t to serve as conditions for the generation process. Notably, we interpolate the valid masks of the partial image and depth into the latent space to guide the model in generating the missing regions. Therefore, in the reverse process, the U-Net’s objective is to predict the noise $\hat{\epsilon}$, conditioned on $z_c = \{z_{i,p}, z_{d,p}, z_{i,m}, z_{d,m}\}$, z_0 and t , where $\{\dots\}$ denotes the concatenation operation, and $z_{i,m}, z_{d,m}$ represent the corresponding latent valid masks. The training loss \mathcal{L} is formulated as follows:

$$\mathcal{L} = \mathbb{E}_{d_0, \epsilon \sim \mathcal{N}(0,1), t \sim U(1,T)} \left[\|\epsilon - \hat{\epsilon}_\theta(z_c, z_0, t)\|^2 \right]. \quad (7)$$

3.4. Scene Embedder

Based on the geometry-appearance dual-stream diffusion, our SceneCompleter can infer a plausible 3D structure (A, G) from the incomplete geometry and appearance clues. However, the problem remains highly ill-posed for large-angle viewpoint changes. To address this, we design a scene embedder, which encodes information from the reference view into the entire process, providing global scene context for 3D scene completion, thereby improving the generation in missing areas. As shown in Figure 1, the core of the Scene Embedder is to use a learnable scene embedding to encode the global information of the scene. Specifically, we first extract the reference view features f_{ref} using a pretrained CLIP image encoder. Then, our learnable scene embedding f_{emb} interacts with these features to obtain the scene information. This process can be described as:

$$f_{\text{scene}} = \text{CrossAttn}(W_q(f_{\text{emb}}), W_k(f_{\text{ref}}), W_v(f_{\text{ref}})), \quad (8)$$

where W_q , W_k , and W_v are the query, key, and value projections, respectively. The scene information f_{scene} is then

used in the U-Net’s cross-attention interaction to incorporate global scene information into the generation process.

3.5. Geometry Alignment and 3D Scene Completion

Since we apply affine-invariant normalization during 3D scene completion, it is necessary to align the completed scene with the original geometry. This alignment can be achieved by matching the incomplete depth clues d_p with the predicted depth \hat{d} . Specifically, we use the valid depth mask M_{d_p} to locate the corresponding predicted depths \hat{d}_p , and then apply a least-squares fitting to align d_p with \hat{d}_p . The optimization for computing the scale and offset is:

$$\text{scale, offset} = \arg \min_{\text{scale, offset}} \|\hat{d}_p - \text{scale} \cdot d_p - \text{offset}\|^2. \quad (9)$$

This process computes the scale and offset, which are then used to restore the missing areas in the scene. The final aligned depth \hat{d}_{aligned} is yielded as follows:

$$\hat{d}_{\text{aligned}} = \text{scale} \cdot \hat{d} + \text{offset}. \quad (10)$$

After obtaining \hat{d}_{aligned} , we can restore it to a 3D pointmap $\hat{\mathbf{X}}_i$ using the camera parameters K_i , R_i , and T_i as follows:

$$\hat{\mathbf{X}}_i = R_i^{-1} K_i^{-1} \tilde{\mathbf{p}}_i \hat{d}_{\text{aligned}} - R_i^{-1} T_i, \quad (11)$$

where $\tilde{\mathbf{p}}_i$ denotes the pixel homogeneous coordinates.

4. Experiments

In this section, we conduct experiments on zero-shot novel view synthesis to demonstrate the effectiveness of the proposed method. We provide both quantitative and qualitative results and provide ablations to analyze our SceneCompleter. Experiments demonstrate that our method shows with both appearance and geometric consistency across multiple datasets.

4.1. Implementation Details

Our model is built upon Stable Diffusion v2 [25]. Following ViewCrafter [35], we trained our model using the DL3DV-10K [14] and RealEstate-10K [37] datasets. Since the two datasets do not provide calibrated depth or other geometric information, we use Dust3R [30] to build our training data. Specifically, we randomly sample five frames from the scene with different strides (1, 2, 4, 8), simulating different viewpoint variations. These five frames are then combined to form a small scene. For each set of five frames, we use Dust3R to estimate their corresponding depth, camera pose, and intrinsics. During training, for each image, we randomly project one of the five frames onto the current frame, using it as input, while the current frame serves as the constraint (including projecting the current frame itself to address the blur issue). We train our model for 50k iterations with an effective batch size of 32 and a learning rate of $3e-5$.

4.2. Zero-shot Novel View Synthesis Comparison

Datasets and Metrics We evaluate our model’s generative novel view synthesis on the zero-shot DL3DV-10K [14], RealEstate-10K [37] test sets, and out-of-distribution datasets Tanks-and-Temples [12] and Co3D [24]. We choose the regression-based method Dust3R, the 2D generative-based methods MotionCtrl, and ViewCrafter as our baselines. For 2D metrics, we use PSNR, SSIM, and LPIPS for evaluation. For 3D metrics, we calculate the camera rotation distance R_{dist} and translation distance T_{dist} as follows:

$$R_{\text{dist}} = \sum_{i=1}^n \arccos\left(\frac{\text{tr}(\mathbf{R}_{\text{gen}}^i \mathbf{R}_{\text{gt}}^{iT}) - 1}{2}\right), \quad (12)$$

$$T_{\text{dist}} = \sum_{i=1}^n \|\mathbf{T}_{\text{gt}}^i - \mathbf{T}_{\text{gen}}^i\|_2, \quad (13)$$

where $\mathbf{R}_{\text{gen}}^i$ and \mathbf{R}_{gt}^i are the predicted and ground truth rotation matrices, respectively, and $\mathbf{T}_{\text{gen}}^i$ and \mathbf{T}_{gt}^i are the predicted and ground truth translation vectors, respectively.

Qualitative comparison. Figure 3 shows the qualitative comparison results of our method. Dust3R [30], being a regression-based method, lacks generative capabilities, resulting in missing areas in the novel view generation. MotionCtrl [31], on the other hand, synthesizes novel views based on a single image and camera trajectory. However, the image itself lacks scale information, leading to a mismatch between the camera trajectory’s scale and the image scale, which makes it difficult to control the new viewpoint. As shown in Figure 3, MotionCtrl often exhibits minimal camera viewpoint changes, leading to inaccurate novel view synthesis. For ViewCrafter [35], which projects the reference view to the novel view and relies on a video generation model to complete the overall image, naturally avoids scale issues by directly using camera projection to obtain the incomplete conditional image. However, by relying solely on RGB input without 3D information, ViewCrafter sometimes struggles to understand scene relationships, resulting in incorrect scene results or the addition/removal of scene content. For example, in the second row, the generated 3D structure appears inconsistent, while in the second-to-last row, an extra wine bottle is erroneously added to the table, conflicting with other viewpoints. Our SceneCompleter, which simultaneously models both geometry and appearance, benefits from structural guidance, ensuring superior 3D consistency. Additionally, our Scene Embedder encodes global scene information, enabling our model to effectively complete large missing regions while preserving consistency with the original structure, even under significant camera viewpoint changes.

Quantitative Comparison. Table 1 presents our quantitative comparison experiments, where we consider both 2D

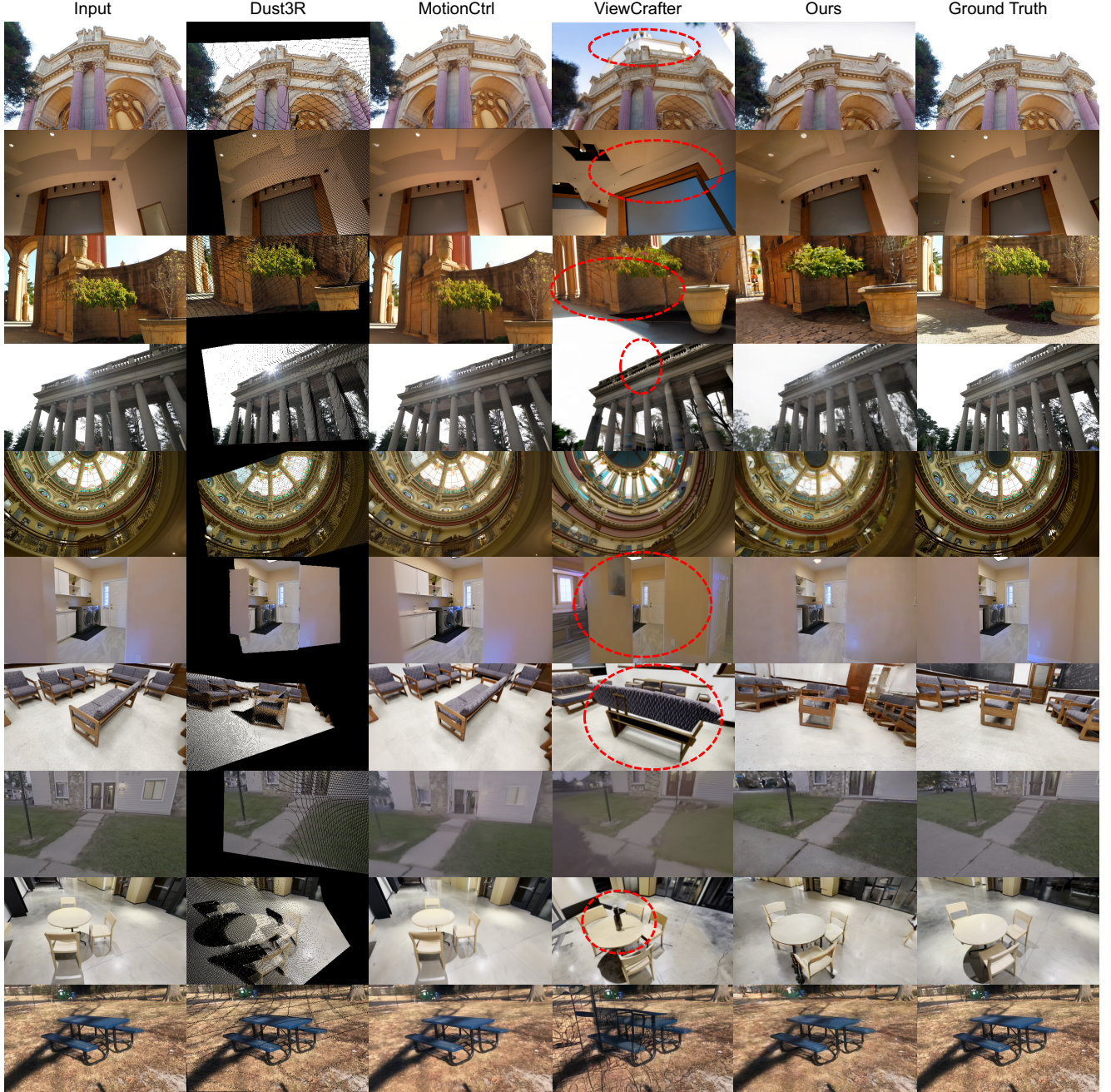


Figure 3. **Qualitative comparison of zero-shot novel view synthesis on Tanks-and-Temples [12], RealEstate10K [37], DL3DV-10K [14], CO3D [24] datasets.** Our SceneCompleter achieves more realistic and 3D-consistent novel view synthesis.

appearance and 3D structure metrics. Additionally, we divide the dataset into an easy set and a hard set for more granular comparisons. In terms of 2D metrics, our model outperforms all others in PSNR and SSIM, primarily due to our joint modeling of both geometry and appearance, which results in more consistent and realistic structures in novel view synthesis. Additionally, we achieve the best LPIPS scores in most cases (except for one), demonstrating that our model not only generates high-quality and geometrically consistent structures but also produces visually realis-

tic appearances in novel view synthesis. In terms of 3D metrics, our method consistently outperforms 2D-based generative methods, thanks to the incorporation of geometry information into the generation process, which ensures more consistent structures. However, our 3D metrics sometimes fall slightly behind the regression-based method, Dust3R. This could be due to some details being filled in the missing areas during generation, which may influence the calculation of 3D metrics.

Table 1. **Quantitative comparison of zero-shot novel view synthesis on Tanks-and-Temples[12], RealEstate10K[37], DL3DV-10K [14] and CO3D[24] dataset.** Our SceneCompleter outperforms baselines across most image quality and pose accuracy metrics.

Dataset	Easy set					Hard set				
	LPIPS ↓	PSNR ↑	SSIM ↑	R_{dist} ↓	T_{dist} ↓	LPIPS ↓	PSNR ↑	SSIM ↑	R_{dist} ↓	T_{dist} ↓
Tanks-and-Temples										
Dust3R [30]	0.478	16.26	0.506	0.173	1.021	0.527	14.74	0.368	0.498	1.125
MotionCtrl [31]	0.415	16.55	0.498	0.222	0.992	0.464	15.52	0.437	0.578	1.384
ViewCrafter [35]	0.217	20.67	0.668	0.213	0.853	0.273	18.50	0.554	0.514	1.200
Ours	0.207	21.43	0.700	0.163	0.828	0.247	19.80	0.555	0.496	1.037
RealEstate10K										
Dust3R [30]	0.689	12.55	0.496	0.046	0.174	0.661	12.31	0.490	0.047	0.169
MotionCtrl [31]	0.102	22.88	0.810	0.116	1.937	0.117	22.56	0.808	0.031	1.051
ViewCrafter [35]	0.141	22.43	0.807	0.021	0.134	0.161	22.01	0.802	0.030	0.149
Ours	0.121	26.03	0.867	0.035	0.121	0.118	25.94	0.868	0.031	0.143
DL3DV-10K										
Dust3R [30]	0.660	13.63	0.429	0.828	1.181	0.741	10.05	0.488	0.819	0.785
MotionCtrl [31]	0.540	16.74	0.657	0.412	1.107	0.585	14.90	0.462	0.822	0.951
ViewCrafter [35]	0.346	22.91	0.697	2.215	1.098	0.426	18.49	0.472	0.821	0.951
Ours	0.192	24.38	0.789	0.369	0.456	0.271	21.25	0.660	0.368	0.640
Co3d										
Dust3R [30]	0.555	13.40	0.284	0.163	1.363	0.595	8.67	0.257	2.334	1.779
MotionCtrl [31]	0.531	11.03	0.147	0.171	1.214	0.394	11.64	0.178	2.607	0.968
ViewCrafter [35]	0.399	15.14	0.263	0.178	1.197	0.548	14.54	0.121	2.610	0.968
Ours	0.378	17.45	0.326	0.168	0.607	0.374	15.07	0.306	2.330	0.607

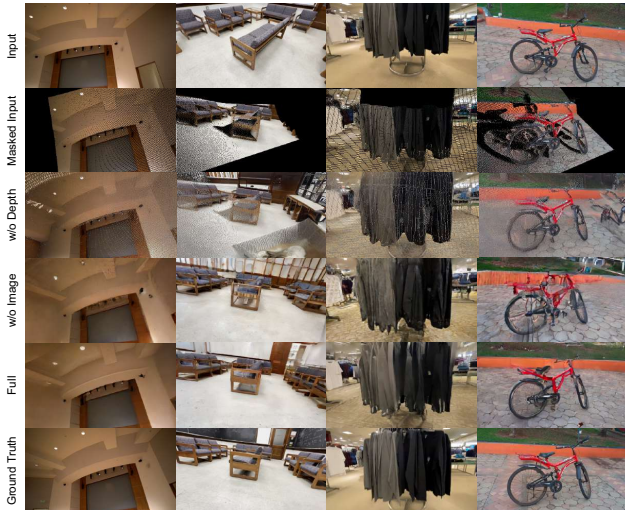


Figure 4. **Ablation on geometry clue and Scene Embedder.** The results demonstrate that the geometry clues play a decisive role in novel view synthesis, while the scene information encoded by the Scene Embedder is crucial for detail recovery.

4.3. 3D Scene Completion

We present our 3D scene completion results in Figure 5. From left to right, we iteratively update and refine the scene information, gradually improving the completion. As shown, leveraging our joint modeling of geometry and appearance, along with our simple yet effective alignment

strategy, Our model achieves iterative and coherent 3D scene completion while preserving the original 3D structure, enabling single-image 3D scene generation. Notably, as illustrated in Figure 5(d), our model adapts not only to camera translation but also to camera rotation, demonstrating its strong robustness.

4.4. Experimental Analysis

In this section, we systematically conduct ablation studies to validate the effectiveness of our design. Specifically, we focus on two crucial components: the joint modeling of geometry and appearance, which ensures structural consistency during 3D scene completion, and the global scene embedder, which provides holistic scene understanding for improved completion quality, especially when large areas of the scene are missing.

Qualitative Results. Figure 4 presents our qualitative ablation study. From the figure, we observe the following key points: 1) Simultaneously modeling geometry is crucial for accurate geometric structure prediction. For example, in the second row, the image after completion still contains significant noise, likely due to the absence of depth information for flat surfaces. Additionally, in the second column, the lack of geometric structure information results in unreasonable floating shadows in the missing areas, which would be even more evident in the depth map as incorrect. 2) The global scene information encoded by the scene embedder

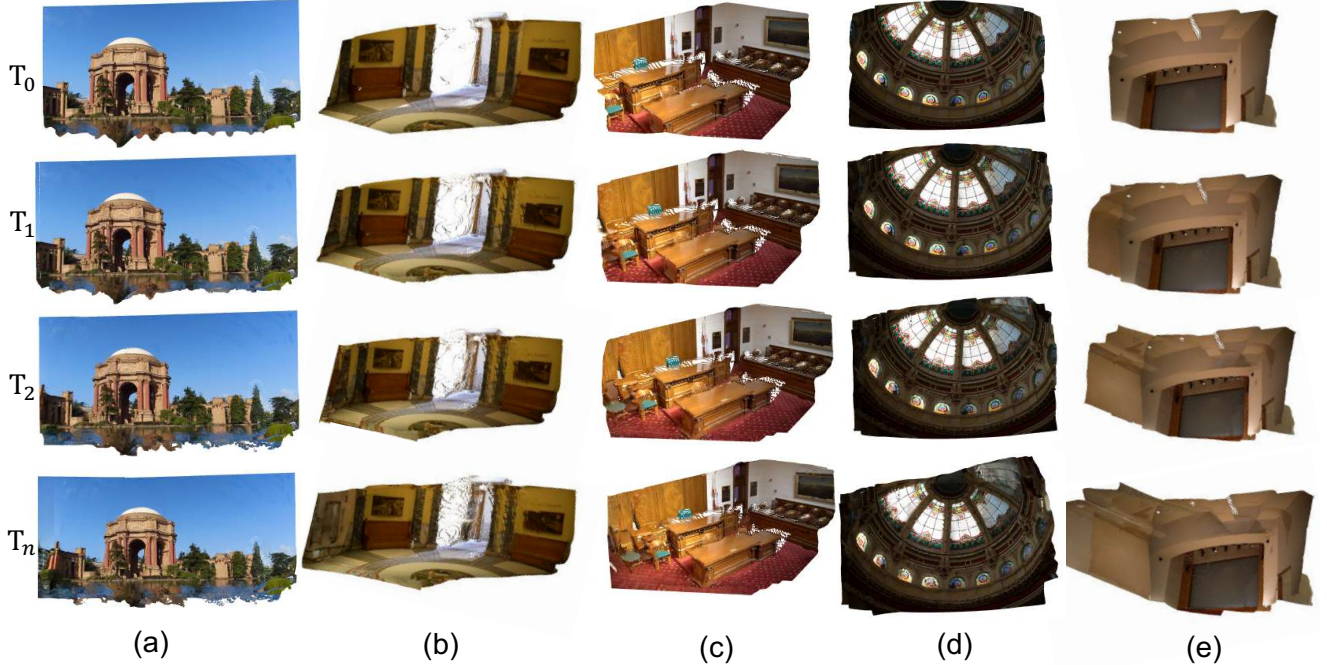


Figure 5. **3D scene completion visualization.** Our SceneCompleter can iteratively refine 3D scenes.

Table 2. **Quantitative ablation on geometry clue and Scene Embedder.** The results demonstrate that both the geometry clue and Scene Embedder play crucial roles in the final outcome.

Dataset	Test set				
	LPIPS ↓	PSNR ↑	SSIM ↑	R_{dist} ↓	T_{dist} ↓
TNT					
w/o depth	0.727	18.82	0.431	2.805	0.920
w/o SE	0.305	21.66	0.798	2.802	0.896
Full	0.275	23.19	0.826	2.790	0.752
Re10K					
w/o depth	0.726	10.92	0.224	0.592	1.246
w/o SE	0.404	15.44	0.484	0.373	1.000
Full	0.391	15.56	0.510	0.369	0.752
DL3DV					
w/o depth	0.810	14.83	0.128	1.993	0.960
w/o SE	0.459	18.28	0.456	2.086	0.948
Full	0.387	19.97	0.506	1.785	0.824
Co3D					
w/o depth	0.586	18.20	0.277	0.387	0.794
w/o SE	0.341	18.18	0.373	0.111	0.287
Full	0.328	19.11	0.420	0.101	0.287

plays a critical role in handling fine details. For instance, in the first column, the beams appear structurally deformed, with their sharp edges lost, and in the fourth row, the bike’s projection information appears messy. When scene information is available, the model can accurately infer the bike’s structure, but in its absence, it generates incorrect structures.

Quantitative Results. Table 2 shows the results of our

quantitative ablation study. As observed, after removing the depth guidance, both 2D and 3D metrics decrease, with significant drops in LPIPS and SSIM. This highlights the importance of modeling geometry for achieving reasonable and structured image completion. Additionally, when the Scene Embedder is ablated, both 2D and 3D metrics show some decline, which aligns with our qualitative analysis, where we observed that the Scene Embedder helps the model handle detailed information more effectively.

5. Conclusion

In this paper, we propose SceneCompleter, a novel framework for achieving 3D consistent generative novel view synthesis through dense 3D scene completion. Our core insight is that by simultaneously modeling geometry and appearance in generative novel view synthesis, the model can more effectively infer 3D structure, leading to more coherent and consistent novel view synthesis. Specifically, we first utilize the powerful stereo reconstruction model Dust3R [30] to extract both geometry and appearance clues from the reference view. These clues are then passed into a Geometry-Appearance Dual-Stream Diffusion, where denoising is performed in the 3D geometry-appearance space (A, G) based on the conditional geometry and appearance clues. Additionally, we design a Scene Embedder to extract global information from the scene for generation, which is particularly important when dealing with large changes in viewpoint or when filling in chaotic missing areas. After denoising and obtaining the completed 3D scene, we align it with the original 3D scene and restore the filled-in re-

gions into the original 3D structure, resulting in a more complete 3D model. Thanks to the simultaneous modeling of geometry and appearance, extensive experiments show that our method achieves high-quality and geometrically consistent zero-shot generative novel view synthesis.

References

- [1] Anh-Quan Cao and Raoul De Charette. Scenerf: Self-supervised monocular 3d scene reconstruction with radiance fields. In *ICCV*, pages 9387–9398, 2023. [1](#)
- [2] David Charatan, Sizhe Lester Li, Andrea Tagliasacchi, and Vincent Sitzmann. pixelsplat: 3d gaussian splats from image pairs for scalable generalizable 3d reconstruction. In *Proceedings of the IEEE/CVF conference on computer vision and pattern recognition*, pages 19457–19467, 2024. [2](#)
- [3] Yuedong Chen, Hao-fei Xu, Chuanxia Zheng, Bohan Zhuang, Marc Pollefeys, Andreas Geiger, Tat-Jen Cham, and Jianfei Cai. Mvsplat: Efficient 3d gaussian splatting from sparse multi-view images. In *European Conference on Computer Vision*, pages 370–386. Springer, 2024. [2](#)
- [4] Hochul Cho, Jangyoon Kim, and Woontack Woo. Novel view synthesis with multiple 360 images for large-scale 6-dof virtual reality system. In *2019 IEEE Conference on Virtual Reality and 3D User Interfaces (VR)*, pages 880–881. IEEE, 2019. [1](#)
- [5] Jaeyoung Chung, Suyoung Lee, Hyeongjin Nam, Jaerin Lee, and Kyoung Mu Lee. Lucidreamer: Domain-free generation of 3d gaussian splatting scenes. *arXiv preprint arXiv:2311.13384*, 2023. [2](#)
- [6] Hao He, Yinghao Xu, Yuwei Guo, Gordon Wetzstein, Bo Dai, Hongsheng Li, and Ceyuan Yang. Cameractrl: Enabling camera control for text-to-video generation. *arXiv preprint arXiv:2404.02101*, 2024. [2](#)
- [7] Jonathan Ho, Ajay Jain, and Pieter Abbeel. Denoising diffusion probabilistic models. *NIPS*, 33:6840–6851, 2020. [2](#)
- [8] Binbin Huang, Zehao Yu, Anpei Chen, Andreas Geiger, and Shenghua Gao. 2d gaussian splatting for geometrically accurate radiance fields. In *ACM SIGGRAPH 2024 conference papers*, pages 1–11, 2024. [2](#)
- [9] Yuanhui Huang, Wenzhao Zheng, Borui Zhang, Jie Zhou, and Jiwen Lu. Selfoc: Self-supervised vision-based 3d occupancy prediction. In *CVPR*, pages 19946–19956, 2024. [1](#)
- [10] Bingxin Ke, Anton Obukhov, Shengyu Huang, Nando Metzger, Rodrigo Caye Daudt, and Konrad Schindler. Repurposing diffusion-based image generators for monocular depth estimation. In *Proceedings of the IEEE/CVF Conference on Computer Vision and Pattern Recognition*, pages 9492–9502, 2024. [4](#)
- [11] Bernhard Kerbl, Georgios Kopanas, Thomas Leimkühler, and George Drettakis. 3d gaussian splatting for real-time radiance field rendering. *ACM Trans. Graph.*, 42(4):139–1, 2023. [1](#), [2](#)
- [12] Arno Knapitsch, Jaesik Park, Qian-Yi Zhou, and Vladlen Koltun. Tanks and temples: Benchmarking large-scale scene reconstruction. *ACM Transactions on Graphics (ToG)*, 36(4):1–13, 2017. [5](#), [6](#), [7](#)
- [13] Vincent Leroy, Yohann Cabon, and Jérôme Revaud. Grounding image matching in 3d with mast3r. In *ECCV*, pages 71–91. Springer, 2024. [2](#)
- [14] Lu Ling, Yichen Sheng, Zhi Tu, Wentian Zhao, Cheng Xin, Kun Wan, Lantao Yu, Qianyu Guo, Zixun Yu, Yawen Lu, et al. D13dv-10k: A large-scale scene dataset for deep learning-based 3d vision. In *Proceedings of the IEEE/CVF Conference on Computer Vision and Pattern Recognition*, pages 22160–22169, 2024. [5](#), [6](#), [7](#)
- [15] Fangfu Liu, Wenqiang Sun, Hanyang Wang, Yikai Wang, Haowen Sun, Junliang Ye, Jun Zhang, and Yueqi Duan. Reconx: Reconstruct any scene from sparse views with video diffusion model. *arXiv preprint arXiv:2408.16767*, 2024. [1](#), [2](#)
- [16] Fangfu Liu, Wenqiang Sun, Hanyang Wang, Yikai Wang, Haowen Sun, Junliang Ye, Jun Zhang, and Yueqi Duan. Reconx: Reconstruct any scene from sparse views with video diffusion model, 2024. [2](#), [3](#)
- [17] Minghua Liu, Chao Xu, Haian Jin, Linghao Chen, Mukund Varma T, Zexiang Xu, and Hao Su. One-2-3-45: Any single image to 3d mesh in 45 seconds without per-shape optimization. *Advances in Neural Information Processing Systems*, 36:22226–22246, 2023. [2](#)
- [18] Ruoshi Liu, Rundi Wu, Basile Van Hoorick, Pavel Tokmakov, Sergey Zakharov, and Carl Vondrick. Zero-1-to-3: Zero-shot one image to 3d object. In *Proceedings of the IEEE/CVF international conference on computer vision*, pages 9298–9309, 2023. [1](#), [2](#)
- [19] Xiaoxiao Long, Yuan-Chen Guo, Cheng Lin, Yuan Liu, Zhiyang Dou, Lingjie Liu, Yuexin Ma, Song-Hai Zhang, Marc Habermann, Christian Theobalt, et al. Wonder3d: Single image to 3d using cross-domain diffusion. In *Proceedings of the IEEE/CVF conference on computer vision and pattern recognition*, pages 9970–9980, 2024. [1](#), [2](#)
- [20] Hao Lu, Tianshuo Xu, Wenzhao Zheng, Yunpeng Zhang, Wei Zhan, Dalong Du, Masayoshi Tomizuka, Kurt Keutzer, and Yingcong Chen. Drivingrecon: Large 4d gaussian reconstruction model for autonomous driving. *arXiv preprint arXiv:2412.09043*, 2024. [1](#)
- [21] Ben Mildenhall, Pratul P Srinivasan, Matthew Tancik, Jonathan T Barron, Ravi Ramamoorthi, and Ren Ng. Nerf: Representing scenes as neural radiance fields for view synthesis. *Communications of the ACM*, 65(1):99–106, 2021. [1](#), [2](#)
- [22] Thomas Müller, Alex Evans, Christoph Schied, and Alexander Keller. Instant neural graphics primitives with a multiresolution hash encoding. *ACM transactions on graphics (TOG)*, 41(4):1–15, 2022. [2](#)
- [23] William Peebles and Saining Xie. Scalable diffusion models with transformers. In *ICCV*, pages 4195–4205, 2023. [2](#)
- [24] Jeremy Reizenstein, Roman Shapovalov, Philipp Henzler, Luca Sbordone, Patrick Labatut, and David Novotny. Common objects in 3d: Large-scale learning and evaluation of real-life 3d category reconstruction. In *Proceedings of the IEEE/CVF international conference on computer vision*, pages 10901–10911, 2021. [5](#), [6](#), [7](#)

- [25] Robin Rombach, Andreas Blattmann, Dominik Lorenz, Patrick Esser, and Björn Ommer. High-resolution image synthesis with latent diffusion models. In *Proceedings of the IEEE/CVF conference on computer vision and pattern recognition*, pages 10684–10695, 2022. [2](#), [3](#), [5](#)
- [26] Robin Rombach, Andreas Blattmann, Dominik Lorenz, Patrick Esser, and Björn Ommer. High-resolution image synthesis with latent diffusion models. In *CVPR*, pages 10684–10695, 2022. [2](#)
- [27] Kyle Sargent, Zizhang Li, Tanmay Shah, Charles Herrmann, Hong-Xing Yu, Yunzhi Zhang, Eric Ryan Chan, Dmitry Lagun, Li Fei-Fei, Deqing Sun, et al. Zeronvs: Zero-shot 360-degree view synthesis from a single image. In *Proceedings of the IEEE/CVF Conference on Computer Vision and Pattern Recognition*, pages 9420–9429, 2024. [2](#)
- [28] Christoph Schuhmann, Romain Beaumont, Richard Vencu, Cade Gordon, Ross Wightman, Mehdi Cherti, Theo Coombes, Aarush Katta, Clayton Mullis, Mitchell Wortsman, et al. Laion-5b: An open large-scale dataset for training next generation image-text models. *Advances in neural information processing systems*, 35:25278–25294, 2022. [3](#)
- [29] Hengyi Wang and Lourdes Agapito. 3d reconstruction with spatial memory. *arXiv preprint arXiv:2408.16061*, 2024. [3](#)
- [30] Shuzhe Wang, Vincent Leroy, Yohann Cabon, Boris Chidlovskii, and Jerome Revaud. Dust3r: Geometric 3d vision made easy. In *Proceedings of the IEEE/CVF Conference on Computer Vision and Pattern Recognition*, pages 20697–20709, 2024. [2](#), [3](#), [5](#), [7](#), [8](#)
- [31] Zhouxia Wang, Ziyang Yuan, Xintao Wang, Yaowei Li, Tianshui Chen, Menghan Xia, Ping Luo, and Ying Shan. Motionctrl: A unified and flexible motion controller for video generation. In *ACM SIGGRAPH 2024 Conference Papers*, pages 1–11, 2024. [2](#), [5](#), [7](#)
- [32] Christopher Wewer, Kevin Raj, Eddy Ilg, Bernt Schiele, and Jan Eric Lenssen. latentsplat: Autoencoding variational gaussians for fast generalizable 3d reconstruction. In *European Conference on Computer Vision*, pages 456–473. Springer, 2024. [2](#)
- [33] Jinbo Xing, Menghan Xia, Yong Zhang, Haoxin Chen, Wangbo Yu, Hanyuan Liu, Gongye Liu, Xintao Wang, Ying Shan, and Tien-Tsin Wong. Dynamicrafter: Animating open-domain images with video diffusion priors. In *ECCV*, pages 399–417. Springer, 2024. [2](#)
- [34] Jianing Yang, Alexander Sax, Kevin J Liang, Mikael Henaff, Hao Tang, Ang Cao, Joyce Chai, Franziska Meier, and Matt Feiszli. Fast3r: Towards 3d reconstruction of 1000+ images in one forward pass. *arXiv preprint arXiv:2501.13928*, 2025. [3](#)
- [35] Wangbo Yu, Jinbo Xing, Li Yuan, Wenbo Hu, Xiaoyu Li, Zhipeng Huang, Xiangjun Gao, Tien-Tsin Wong, Ying Shan, and Yonghong Tian. Viewcrafter: Taming video diffusion models for high-fidelity novel view synthesis, 2024. [2](#), [3](#), [5](#), [7](#)
- [36] Wenzhao Zheng, Weiliang Chen, Yuanhui Huang, Borui Zhang, Yueqi Duan, and Jiwen Lu. Occworld: Learning a 3d occupancy world model for autonomous driving. In *European conference on computer vision*, pages 55–72. Springer, 2024. [1](#)
- [37] Tinghui Zhou, Richard Tucker, John Flynn, Graham Fyffe, and Noah Snavely. Stereo magnification: Learning view synthesis using multiplane images. *arXiv preprint arXiv:1805.09817*, 2018. [5](#), [6](#), [7](#)